

DEVELOPMENT OF MAGNETORHEOLOGICAL BRAKE WITH TWO COILS PLACED ON EACH SIDE OF THE BRAKE HOUSING

Nguyen Quoc Hung^{1,2,*}, Nguyen Ngoc Diep², Nguyen Si Dzung^{1,2}

¹Ton Duc Thang University, Ho Chi Minh City, Vietnam

²Industrial University of Ho Chi Minh City, Vietnam

*E-mail: nguyenquochung@tdt.edu.vn

Received February 18, 2015

Abstract. In this study a new configuration of magneto-rheological brake (MRB) with two coils placed on each side of the brake housing is proposed, optimally designed and evaluated. With this configuration, the MRB is expected to provide higher braking torque, more compact size than traditional MRB. After describing an introduction of the proposed configuration, braking torque of the proposed MRB is analyzed based on Bingham-plastic rheological model of magnetorheological fluid (MRF). The optimization of the proposed MRB, the MRB with one coil placed on each side of the brake housing and the conventional MRB is then performed considering maximum braking torque and mass of the brakes. Based on the optimal results, advanced performance characteristics of the proposed MRB are figured out.

Keywords: Magnetorheological fluid (MRF), MR brake, optimal design, disc-type MR brake.

1. INTRODUCTION

In recent years, there have been many researches on development and improvement of magnetorheological brake (MRB), and its application in industry. In comparison with conventional mechanical brakes, the MRBs possess several advantages such as more compact size, fast response, less wearing (there is no dry friction) and capability to accurately control braking torque. Therefore, the MRBs have many potential applications in automatic systems such as robotics, haptic systems, etc. Essentially, in a MRB, the gap between the rotor and the stationary housing is filled up with magnetorheological fluid (MRF), called MRF duct. In the absence of magnetic field, the MRF behaves like a Newtonian fluid which induces a small friction torque to the rotor. When a magnetic field is created with magnetic fluxes going across the MRF duct, the MRF passes from a Newtonian-like fluid to a viscoplastic-like fluid with high controllable shear yield stress in few milliseconds [1]. The high controllable shear yield stress results in a controllable

braking torque of the MRB. In order to improve performance of MRBs, many MRB types have been proposed and evaluated such as disc-type MRB [2–5], drum-type MRBs [6, 7], hybrid-type MRB (a combination of disc-type and drum type MRB) with T-shaped rotor [8, 9]. Recently, Nguyen et al. [10] have proposed a new configuration of MRBs in which magnetic coils are placed directly on both sides of the housing of the MRB. The simulation results showed that with this configuration, some disadvantages of the traditional MRBs such as “bottle-neck” problem of magnetic flux, a nonmagnetic bobbin is required, and difficulties in manufacturing and maintenance can be eliminated. However, that study considered only the MRB with one magnetic coil placed on each side of the housing.

The main technical contribution of this work is to develop and investigate a new configuration of MRB with two magnetic coils placed on each side of the brake housing. The main technical contribution is validated by comparing performance between the proposed and previously developed MRBs. After an introduction of the new configuration of MRBs, the braking torque is derived based on Bingham-plastic behavior of MRF. Subsequently, optimal design of the MRBs is considered. The optimization problem is to find optimal value of significant geometric dimensions of the MRB that can produce a certain required braking torque while the MRB mass is minimized. A finite element analysis integrated with an optimization tool is employed to obtain optimal solutions of the MRBs. From the results, performance characteristics of the proposed MRB are investigated and compared with performance characteristics of the conventional disc-type MRB and the MRB with one magnetic coil placed on each side of the housing.

2. THE MRB WITH TWO COILS PLACED ON EACH SIDE OF THE HOUSING

In this study, a configuration of a disc-type MRB with two coils placed on each side of the brake housing is introduced and its braking torque is analyzed based on Bingham-plastic model of MRF. Fig. 1a shows the previously developed MRB with one coil placed on each side of the housing [10] while Fig. 1b shows the configuration of the proposed MRB with two coils placed on each side of the housing. As shown in the figures, a disc (rotor) made of magnetic steel is fastened to the flange of the MRB shaft made of nonmagnetic steel. The disc is embedded inside a stationary envelop (housing) made of magnetic steel. In Fig. 1a, one wire-coil is directly placed on each side of the housing (in this study, this is referred as single side-coil MRB) while two wire-coils are placed on each side of the housing in Fig. 1b (In this study, this is referred as double side-coil MRB). It is worthy to remark that firstly the coils are wound on a suitable cylinder outside, and then they are covered by adhesive to prevent MRF flow into the coils. The coils are then placed in the housings. The space between the rotary disc and the housing is filled with MRF. In order to prevent the leaking of MRF, radial lip seals are employed. As counter electric currents are applied to the coils as shown in the figures, magnetic fields are generated and the MRF in the gap between the disc and the housing becomes solid-like instantaneously. This results in a controllable friction from the solidified MRF to the rotary disc to slow down and stop the shaft. By using two coils on each side of the housing, a stronger and more uniform magnetic flux density across the MRF ducts is expected and a better performance of the MRB can be obtained.

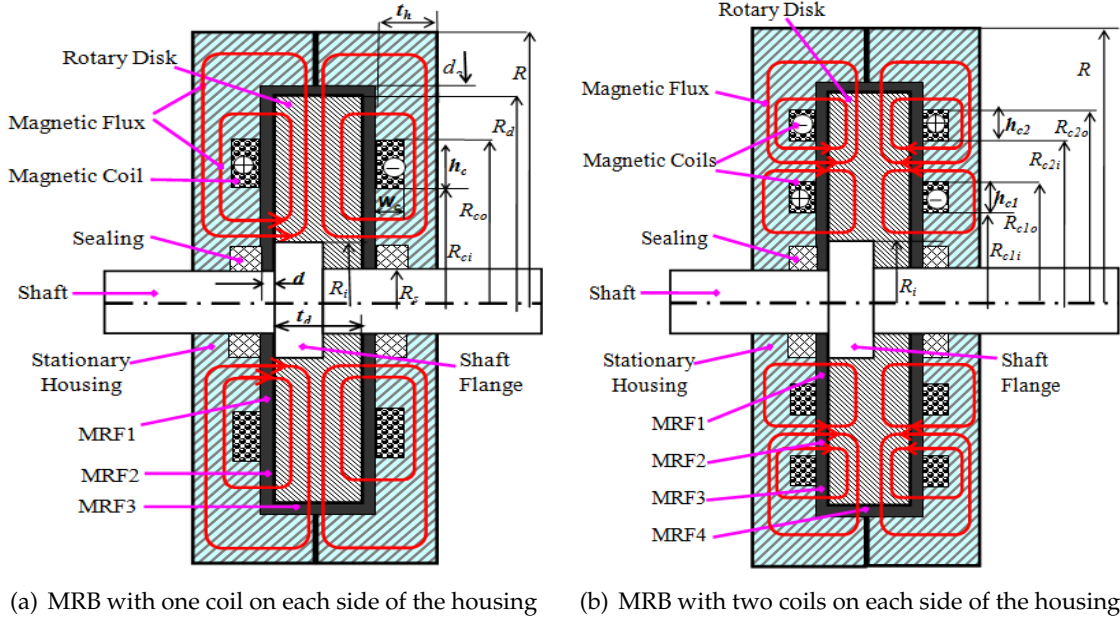


Fig. 1. Configuration of the side-coil MRBs

By assuming that the MRF rheologically behaves as Bingham plastic fluids and by the assumption of a linear velocity profile in the MRF ducts of the brake, the induced braking torque of the single side-coil MRB and the proposed double side-coil MRB can be respectively determined as follows [10–12]

$$T_s = \frac{\pi\mu_{s1}R_{ci}^4}{d} \left[1 - \left(\frac{R_i}{R_{ci}} \right)^4 \right] \Omega + \frac{4\pi\tau_{ys1}}{3} (R_{ci}^3 - R_i^3) + \frac{\pi\mu_{s2}R_d^4}{d} \left[1 - \left(\frac{R_{co}}{R_d} \right)^4 \right] \Omega + \frac{4\pi\tau_{ys2}}{3} (R_d^3 - R_{co}^3) + 2\pi R_d^2 t_d (\tau_{ys3} + \mu_{s3} \frac{\Omega R_d}{d_o}) + 2T_{sf} , \quad (1)$$

$$T_d = \frac{\pi\mu_{d1}R_{ci}^4}{d} \left[1 - \left(\frac{R_i}{R_{ci}} \right)^4 \right] \Omega + \frac{4\pi\tau_{yd1}}{3} (R_{ci}^3 - R_i^3) + \frac{\pi\mu_{d2}R_{c2i}^4}{d} \left[1 - \left(\frac{R_{c1o}}{R_{c2i}} \right)^4 \right] \Omega + \frac{4\pi\tau_{yd2}}{3} (R_{c2i}^3 - R_{c1o}^3) + \frac{\pi\mu_{d3}R_d^4}{d} \left[1 - \left(\frac{R_{c2o}}{R_d} \right)^4 \right] \Omega + \frac{4\pi\tau_{yd3}}{3} (R_d^3 - R_{c2o}^3) + 2\pi R_d^2 t_d (\tau_{yd4} + \mu_{d4} \frac{\Omega R_d}{d_o}) + 2T_{sf} , \quad (2)$$

and the off-state torque (the torque of the MRB when no current is applied to the coil) of both the MRBs can be determined by

$$T_0 = \frac{\pi\mu_0 R_d^4}{d} \left[1 - \left(\frac{R_s}{R_d} \right)^4 \right] \Omega + \frac{4\pi\tau_{y0}}{3} (R_d^3 - R_s^3) + 2\pi R_d^2 t_d (\tau_{y0} + \mu_0 \frac{\Omega R_d}{d_o}) + 2T_{sf} , \quad (3)$$

In the above, R_d is the outer radius of the disc, R_i is the inner radius of the active MRF volume in the end-face duct which is almost equal to the outer radius of the shaft flange, R_s is the shaft diameter at the sealing, d is the gap size of the end-face MRF ducts between the disc and the housing, d_o is the gap size of the annular MRF duct at the outer cylindrical face of the disc, t_d is the thickness of the disc, Ω is the angular velocity of the

rotor, T_{sf} is the friction torque between the shaft of the brake and the sealing, R_{ci} and R_{co} are the inner and outer radius of the coil in case of the single side-coil MRB, R_{c1i} and R_{c1o} are the inner and outer radius of the inner coil while R_{c2i} and R_{c2o} are the inner and outer radius of the outer coil in case of the double side-coil MRB. μ_{s1} , μ_{s2} and μ_{s3} are respectively the average post yield viscosity of MRF denoted by MRF1, MRF2 and MRF3 in case of the single side-coil MRB while τ_{s1} , τ_{s2} and τ_{s3} are the corresponding yield stress. μ_{d1} , μ_{d2} , μ_{d3} and μ_{d4} are respectively the average post yield viscosity of MRF denoted by MRF1, MRF2, MRF3 and MRF4 in case of the double side-coil MRB while τ_{d1} , τ_{d2} , τ_{d3} and τ_{d4} are the corresponding yield stress. τ_{y0} and μ_0 are the zero-field yield stress and viscosity of the MRF. It is noted that the induced yield stress and post yield viscosity of the MRF are dependent on the exerted magnetic flux density across the ducts of MRF as reported in several researches [13,14].

The lip seal friction torque T_{sf} can be approximately calculated by [15]

$$T_{sf} = 0.65(2R_s)^2\Omega^{1/3}. \quad (4)$$

In the above, T_{sf} is the friction torque of a lip seal in ounce-inches, Ω is the rotation speed of the brake shaft measured in rounds per minute, and R_s is the shaft diameter at the sealing measured in inches.

3. OPTIMAL DESIGN OF MRBS

In this study, optimization of the abovementioned MRBs is considered. In design of MRBs, besides the braking torque, another issue that should be taken into account is their mass. It is obvious that the mass of the MRBs should be as small as possible to reduce the MRB size and cost. In addition, smaller mass of the MRBs can reduce the effect of inertia in some application such as robotics, haptic systems. Therefore, the objective of the optimization in this study is to find optimal value of significant geometric dimensions of the MRB that can produce a certain required braking torque while the MRB mass is minimized. Generally, the MRB mass can be approximately calculated by

$$m_b = V_d\rho_d + V_h\rho_h + V_s\rho_s + V_{MR}\rho_{MR} + V_c\rho_c, \quad (5)$$

where V_d , V_h , V_s , V_{MR} and V_c are respectively the geometric volume of the disc, the housing, the shaft, the MRF and the coil of the brake. These parameters are functions of geometric dimensions of the MRB structures, which vary during the optimization process. ρ_d , ρ_h , ρ_s , ρ_{MR} , and ρ_c are density of the discs, the housing, the shaft, the MRF and the coil material, respectively. From the above, the optimization design problem of the MRBs in this study can be summarized as follows: *Find optimal value of significant dimensions of the MRBs so that the brake mass determined by Eq. (5) is minimized, while its maximum braking torque determined by Eqs. (1) and (2) is constrained to be greater than a required braking torque.*

In order to determine the braking torque of the MRB using Eqs. (1) and (2), firstly, the magnetic density across the MRF ducts of the MRB must be determined. In order to obtain magnetic solution of the MRF based device, both approximate analytical method and finite element method (FEM) can be used [16, 17]. In this research, for more accurate solution, FEM is used. In this study, finite element models using 2D-axisymmetric

couple element (PLANE 13) of commercial ANSYS software are employed to solve magnetic circuits of the MRB. On obtaining the magnetic density across the MRF ducts, the rheological parameters of MRF in the ducts such as the yield stress and the post yield viscosity can be calculated. The braking torque of the brake can be then determined from Eqs. (1) and (2). The mass of the MRBs is also determined from their CAD model in the ANSYS software. The FE models used in this study are shown in Fig. 2.

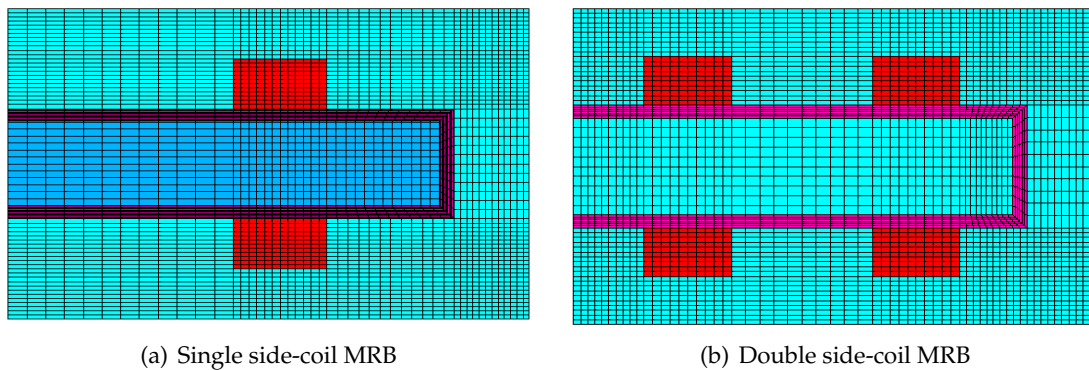


Fig. 2. Finite element model to analyze magnetic circuit of the MRBs

In the FE models, quadrilateral mapped meshing is employed. The meshing size is determined by the number of elements per line (NoEPL). In this study, with an accuracy of 1%, the NoEPL is set by 12. The accuracy of magnetic density as a function of the NoEPL is shown in Figs. 3 and 4. In the figures, B_1 , B_2 , B_3 and B_4 represent the magnetic flux density across the MRF ducts MRF₁, MRF₂, MRF₃, MRF₄ as shown in Fig. 1. From the figures, it can be observed that the accuracy of magnetic density across the MRF ducts is up to 1% or smaller when the NoEPL is increased to 12 or greater. With the NoEPL of 12, the number of elements in case of single coil MRB is 3888 elements while that in case of the double coil is 5904.

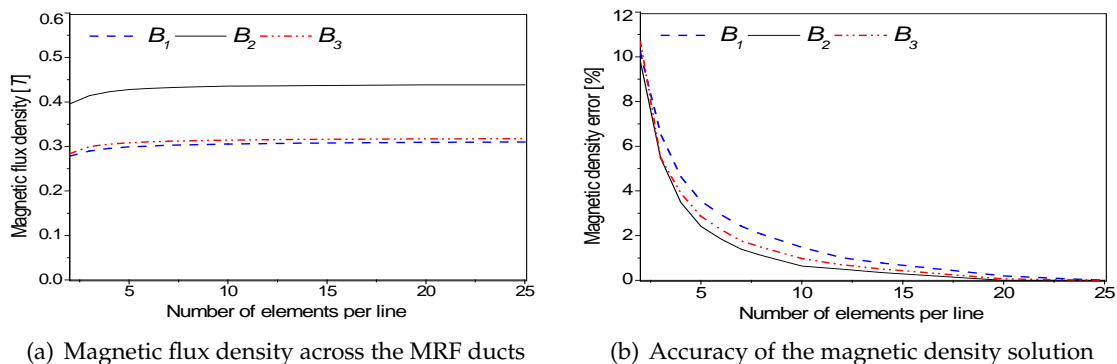


Fig. 3. Accuracy of FE solution as a function of NoEP in case of single side-coil MRB

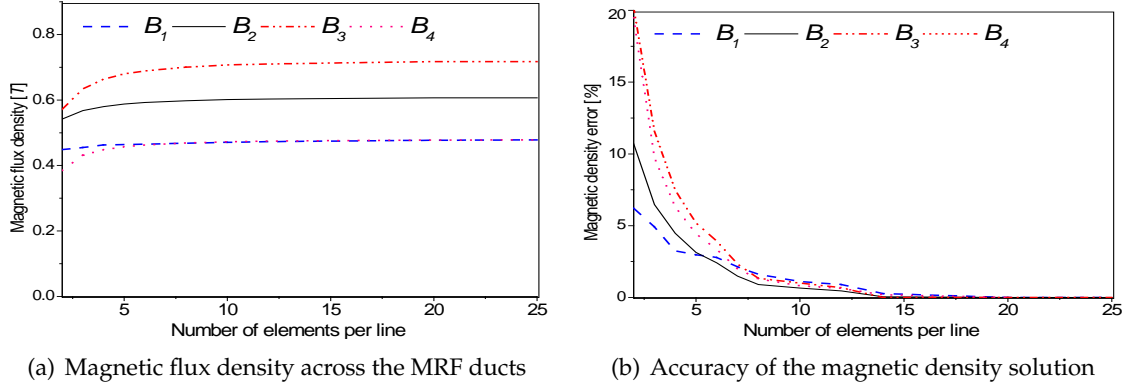


Fig. 4. Accuracy of FE solution as a function of NoEPL in case of double side-coil MRB

4. RESULTS AND DISCUSSIONS

In this section, optimal solutions of the above MRBs are obtained and presented with discussion. It is assumed that the commercial silicon steel is used for magnetic components of the MRB such as the housing and the disc. The coil wires are sized as 21-gage (diameter = 0511 mm) whose maximum working current is around 3A and during the optimization process, a current of 2.5A is applied to the coil. It is noteworthy that the cross section area of the coil is assumed to be fully wounded. In addition, the commercial MRF, MRF132-DG, made by Lord Corporation is used in this research. The Magnetic properties of the brake components are given in Tab. 1 and Fig. 5. The rheological parameters of the MRF132-DG determined from experimental results using curve fitting method are as the followings: $\mu_0 = 0.1pa \cdot s$; $\mu_\infty = 3.8pa \cdot s$; $\alpha_{s\mu} = 4.5T^{-1}$; $\tau_{y0} = 15pa$; $\tau_{y\infty} = 40000pa$; $\alpha_{sty} = 2.9T^{-1}$.

Table 1. Magnetic properties of the MRBs' components

Material	Relative Permeability	Magnetic saturation	Density (kg/m^3)
Silicon Steel	B-H curve (Fig. 5a)	1.55 Tesla	7800
Copper	1		8000
MRF132-DG	B-H curve (Fig. 5b)	1.65 Tesla	2300

In order to find optimal solution, the first order optimization method using the gradient decent algorithm is employed. A detailed description of this algorithm integrated with ANSYS software is mentioned in several researches [16–19]. In the optimization, the following significant geometric dimensions of the MRBs are selected as design variables: The coil height (h_c, h_{c1}, h_{c2}), the coil width (w_c, w_{c1}, w_{c2}), the inner radius of the coils (R_{ci}, R_{ci1}, R_{ci2}), the outer radius of the shaft flange R_i , the outer radius of the disc R_d , the disc thickness t_d , the outer radius of the MRB R and the housing thickness t_h . It is noted that the smaller gap size of the MRF ducts is, the greater braking torque can be produced.

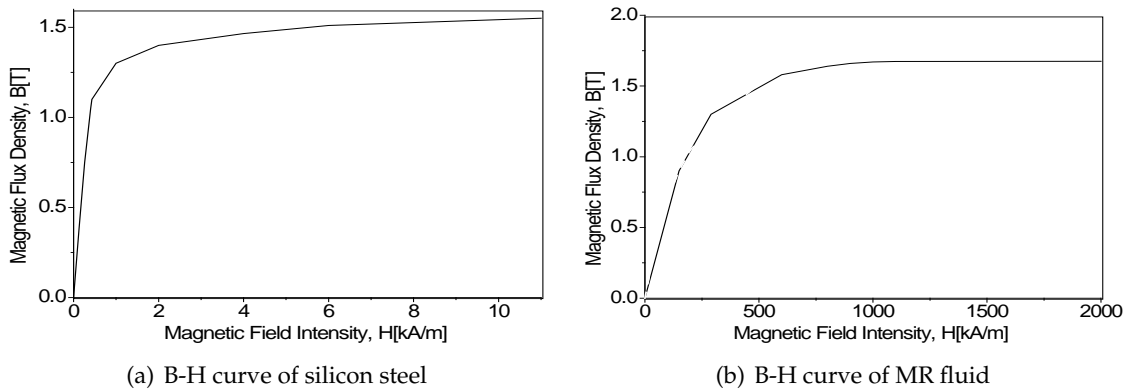


Fig. 5. Magnetic properties of silicon steel and MR fluids

However, the small gap size may result in a large value of the off-state braking torque that degrades performances of the MRBs such as high dissipated energy and overheat. Moreover, the difficulty in manufacturing due to small gap size of the MRF ducts is also an important issue should be taken into consideration. Therefore, in the optimization, the MRF gap size is not considered as a design variable.

Fig. 6 and Fig. 7 show the optimal solution of the single side-coil MRB and the proposed double side-coil MRB, respectively. In this case, the braking torque is constrained to be greater than 10 Nm with 2% of accuracy, the convergence rate is set by 0.1% and the gap size of MRF ducts is set by 0.8 mm. In addition, the shaft radius is set by $R_s = 6$ mm considering the strength of the shaft. The optimal solution of the MRBs is shown in Tab. 2.

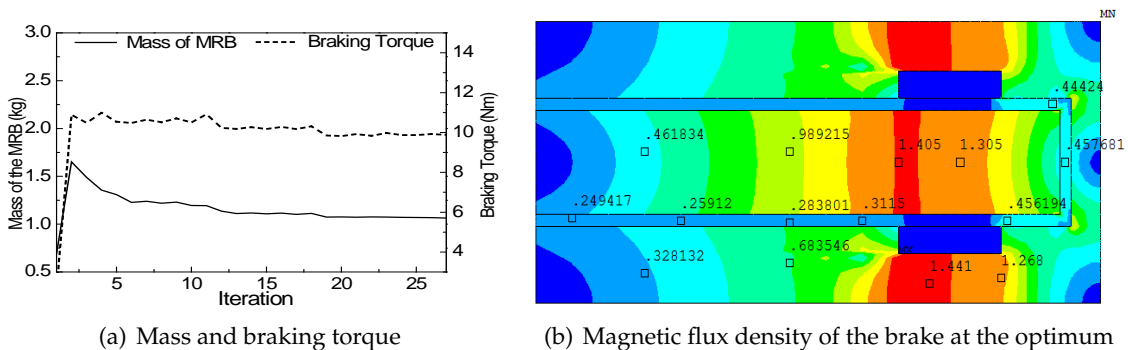


Fig. 6. Optimization solution of the single side-coil MRB

As shown in the figures, at the optimum, braking torque of the MRBs can reach up to 10 Nm as constrained and the mass of the optimized double side-coil MRB 0.82 kg which is significantly smaller than that of the optimized single side-coil MRB, 1.17 kg. It is noteworthy to remark that, with the same constrained braking torque, the mass of the conventional MRB (the MRB with magnetic coil placed in the middle of the housing) is 1.45 kg [10].

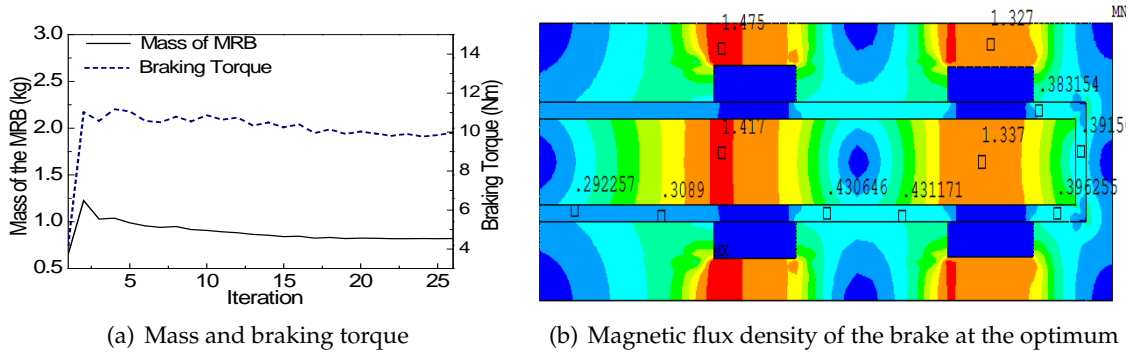


Fig. 7. Optimization solution of the double side-coil MRB

Table 2. Significant parameters of the MRB prototypes

MRB types	Design parameter (mm)	Performance
Single coil	Coil: Width $w_c = 1.7$; Height $h_c = 7$; Radius $R_{ci} = 37$; No. of turns: 2×56 Housing: $R_s = 6, R = 51, t_h = 4.8, L = 18$ Disc: Radius $R_i = 12.5, R_d = 48$; Thickness $t_d = 6.5$ MRF duct gap: 0.8	Max. Torque: 10 Nm Mass: 1.07 kg Off-state Torque: 0.275 Nm Power Cons.: 15W Coil Resistance (Ω): $R_c = 1.2$
Double coil	Coil: Width $w_{c1} \cong w_{c2} = 1.7$; Height $h_{c1} \cong h_{c2} = 6.2$; Radius $R_{c1i} = 23, R_{c2i} = 40$; No. of turns: 4×50 Housing: $R_s = 6, R = 53, t_h = 3.7, L = 13$ Disc: Radius $R_i = 10, R_d = 50$; Thickness $t_d = 4$ MRF duct gap: 0.8	Max. Torque: 10 Nm Mass: 0.82 kg Off-state Torque: 0.243 Nm Power Cons.: 24W Coil Resistance(Ω): $R_{c1} = 0.7,$ $R_{c2} = 1.2$

Fig. 8 shows the mass, the off-state torque and power consumption of the optimized MRBs at different values of the constrained braking torque. From Fig. 8a, it is found that the mass of the proposed double side-coil MRB is always smaller than single side-coil and the conventional MRBs at different values of the required braking torque. From Fig. 8b it is observed that the off-state torque of the double side-coil MRB is smaller than that of the single side coil and conventional ones in case the required braking torque is smaller than 15 Nm. However, when the required braking torque is greater than 15 Nm, the off-state torque of the double side-coil MRB becomes greater. The reason is that in case of double side coil MRB, with two coils on each side, the bottle-neck problem is significantly reduced and magnetic flux energy is strong enough for a larger MRF duct. Thus, the disc radius of the optimized double side-coil MRB is greater than that of the

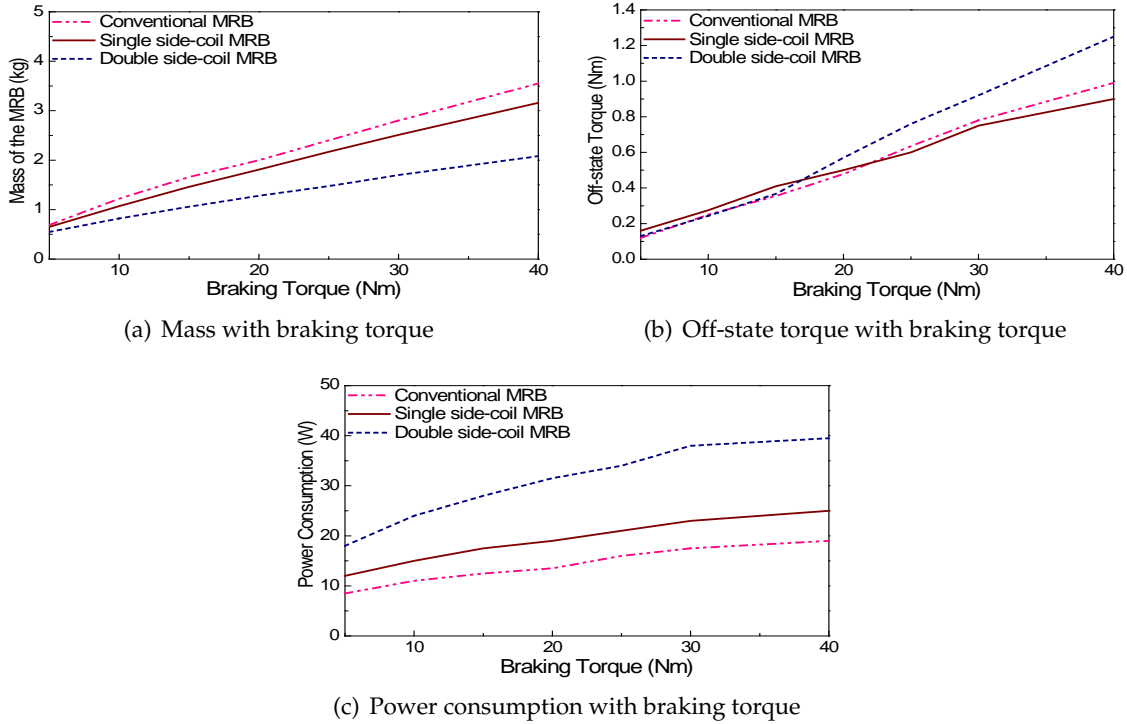


Fig. 8. Optimal results of the MRBs as a function of maximum braking torque

single side coil and conventional ones. This results in a high off-state torque in case of the double side-coil MRB at high braking torque. In some applications where the off-state torque is important such as brakes for automobiles and haptic systems, the off-state torque should be taken into consideration in the optimization as a state variable or in term of a multi-objective function. It is noted that due to bottle-neck problem and magnetic flux energy, the thickness of the housing and the disc in case of the single side-coil and conventional MRBs cannot be very small. This is the reason why the mass of these MRBs at the optimum is greater than that of the double side-coil one. Fig. 8c shows the power consumption of the optimized MRBs at different value of the constrained braking torque. From the figure, it can be seen that the power consumption of the double side-coil MRB is significantly greater than that of the single side-coil and the conventional MRBs. It is obviously because in case of the double side-coil MRB totally four coils are used while the number of coils in case of the single side-coil and conventional MRBs are respectively two coils and one coil. Therefore, in optimal design of MRB, the trade of between the mass reduction and the power consumption of the MRBs should be considered. For applications where the power consumption is not a challenge but the mass reduction is very significant, the double side-coil MRB should be used and vice versa. A multi objective function can also be used in the optimization to take into account the trade-off of these factors [19,20].

5. CONCLUSIONS

In this research work, a new configuration of magneto-rheological brake (MRB) with two coils placed on each side of the housing was proposed. With this configuration, the bottle-neck problem of the brake magnetic circuits can be significantly reduced and a more compact MRB is expected. After an introduction of the new configuration of MRBs, the braking torque was derived based on Bingham-plastic behavior of MRF. Subsequently, optimal design based on finite element analysis of the MRBs was conducted to find optimal value of significant geometric dimensions of the MRB that can produce a certain required braking torque while the MRB mass is minimized. From the results, it was shown that by using the proposed configuration with two coils placed on each side of the housing, the mass of MRB was significantly reduced compared to the MRB with one coil placed on each side of the housing and the conventional MRB. However, the power consumption of the proposed MRB is significantly greater. In addition, the off-state torque of the proposed MRB is greater than that of the MRB with one coil placed on each side of the housing and the conventional MRB when the required braking torque is greater than 15 Nm. As the second phase of this research, the MRBs with more than two coils placed on each side of the housing will be considered and experiment work will be performed for validation. In addition, the power and off-state torque will be considered during the optimization process.

ACKNOWLEDGEMENT

This work was supported by the Vietnam National Foundation for Science and Technology Development (NAFOSTED) under grant no. 107.01-2013.05.

REFERENCES

- [1] A. G. Olabi and A. Grunwald. Design and application of magneto-rheological fluid. *Materials & Design*, **28**, (10), (2007), pp. 2658–2664.
- [2] R. Jacob. Magnetic fluid torque and force transmitting device. US Patent 2,575,360, (1951).
- [3] J. An and D. S. Kwon. Modeling of a magnetorheological actuator including magnetic hysteresis. *Journal of Intelligent Material Systems and Structures*, **14**, (9), (2003), pp. 541–550.
- [4] E. J. Park, D. Stoikov, L. F. da Luz, and A. Suleman. A performance evaluation of an automotive magnetorheological brake design with a sliding mode controller. *Mechatronics*, **16**, (7), (2006), pp. 405–416.
- [5] B. Liu, W. H. Li, P. B. Kosasih, and X. Z. Zhang. Development of an MR-brake-based haptic device. *Smart Materials and Structures*, **15**, (6), (2006), pp. 1960–1969.
- [6] J. Huang, J. Q. Zhang, Y. Yang, and Y. Q. Wei. Analysis and design of a cylindrical magneto-rheological fluid brake. *Journal of Materials Processing Technology*, **129**, (1), (2002), pp. 559–562.
- [7] A. L. Smith, J. C. Ulicny, and L. C. Kennedy. Magnetorheological fluid fan drive for trucks. *Journal of Intelligent Material Systems and Structures*, **18**, (12), (2007), pp. 1131–1136.
- [8] Q. H. Nguyen and S. B. Choi. Optimal design of a T-shaped drum-type brake for motorcycle utilizing magnetorheological fluid. *Mechanics Based Design of Structures and Machines*, **40**, (2), (2012), pp. 153–162.

- [9] Q. H. Nguyen and S. B. Choi. Optimal design of a novel hybrid MR brake for motorcycles considering axial and radial magnetic flux. *Smart Materials and Structures*, **21**, (5), (2012). DOI: 10.1088/0964-1726/21/5/055003.
- [10] Q. H. Nguyen, N. D. Nguyen, and S. B. Choi. Optimal design of a novel configuration of MR brake with coils placed on side housings. In *SPIE Smart Structures and Materials + Nondestructive Evaluation and Health Monitoring*. International Society for Optics and Photonics, (2014). DOI:10.1117/12.2044561.
- [11] Q. H. Nguyen, V. T. Lang, N. D. Nguyen, and S. B. Choi. Geometric optimal design of a magneto-rheological brake considering different shapes for the brake envelope. *Smart Materials and Structures*, **23**, (1), (2014). DOI: 10.1088/0964-1726/23/1/015020.
- [12] Q. H. Nguyen and S. B. Choi. Optimal design of an automotive magnetorheological brake considering geometric dimensions and zero-field friction heat. *Smart Materials and Structures*, **19**, (11), (2010). DOI: 10.1088/0964-1726/19/11/115024.
- [13] M. Zubieta, S. Eceolaza, M. J. Elejabarrieta, and M. M. Bou-Ali. Magnetorheological fluids: characterization and modeling of magnetization. *Smart Materials and Structures*, **18**, (9), (2009), p. 095019. DOI: 10.1088/0964-1726/18/9/095019.
- [14] Q. H. Nguyen and S. B. Choi. Optimal design of an automotive magnetorheological brake considering geometric dimensions and zero-field friction heat. *Smart Materials and Structures*, **19**, (11), (2010). DOI: 10.1088/0964-1726/19/11/115024.
- [15] EPS Division. *Rotary seal design guide*. Parker Hannifin Corporation, Catalog EPS 5350/USA, (2006).
- [16] Q. H. Nguyen, S. B. Choi, Y. S. Lee, and M. S. Han. An analytical method for optimal design of MR valve structures. *Smart Materials and Structures*, **18**, (9), (2009). DOI: 10.1088/0964-1726/18/9/095032.
- [17] Q. H. Nguyen and S. B. Choi. *Optimal design methodology of magnetorheological fluid based mechanisms*, chapter 14, pp. 383–424. INTECH Open Access Publisher, (2012).
- [18] Q. H. Nguyen, Y. M. Han, S. B. Choi, and N. M. Wereley. Geometry optimization of MR valves constrained in a specific volume using the finite element method. *Smart Materials and Structures*, **16**, (6), (2007), pp. 2242–2252.
- [19] Q. H. Nguyen and S. B. Choi. Optimal design of a vehicle magnetorheological damper considering the damping force and dynamic range. *Smart Materials and Structures*, **18**, (1), (2009). DOI: 10.1088/0964-1726/18/1/015013.
- [20] E. J. Park, L. F. da Luz, and A. Suleman. Multidisciplinary design optimization of an automotive magnetorheological brake design. *Computers & Structures*, **86**, (3), (2008), pp. 207–216.